J. Chem. Sci. (2021)133:102
https://doi.org/10.1007/s12039-021-01958-7

REGULAR ARTICLE

Special Issue on Beyond Classical Chemistry

Photo-induced energy and electron transfer in carboxylic acid functionalized bis(4′-*tert*-butylbiphenyl-4-yl)aniline (BBA)-substituted A_3B zinc porphyrins

SUNEEL GANGADA[a], POOJA[b], ANJAIAH BOLIGORLA[b], VIJENDAR REDDY KARLA[b], SRIKANTH BANDI[b], RAVINDER PAWAR[b] and RAGHU CHITTA[a,b,*]

[a]Department of Chemistry, School of Chemical Sciences and Pharmacy, Central University of Rajasthan, Tehsil: Kishangarh, Bandarsindri, District Ajmer Rajasthan 305817, India
[b]Department of Chemistry, National Institute of Technology Warangal, Hanamkonda, Warangal 506004, India
E-mail: raghuchitta@nitw.ac.in; raghuchitta@curaj.ac.in

MS received 31 March 2021; revised 15 June 2021; accepted 5 July 2021

Abstract. Three bis(4′-*tert*-butylbiphenyl-4-yl)aniline (BBA)-substituted A_3B zinc porphyrins containing BBA attached to the three meso-positions of the porphyrin macrocycle via varied spacers i.e., directly connected, phenyl, and ethoxy phenyl, and carboxylic acid functional group at the other meso-position, were synthesized and fully characterized using ^{1}H, ^{13}C NMR, MALDI-TOF, HRMS (ESI+), UV-visible and fluorescence techniques. The steady-state absorption spectrum of **Tetrad-1** revealed bathochromically shifted peaks indicating notable interactions between BBA and ZnP moieties while the interactions were gradually decreased in the case of **Tetrad-2** and **Tetrad-3** due to the introduction of the phenyl and ethoxy phenyl spacer between the chromophores. Steady-state fluorescence studies have revealed that the selective excitation of the BBA moiety at 352 nm in the tetrads resulted in the quenched BBA emission at 395 nm followed by the appearance of the porphyrin emission at 618 or 605 nm indicating the occurrence of photo-induced energy transfer (PEnT) from singlet excited BBA to ZnP i.e., $^1(BBA)_3^*$-ZnP-$CO_2H \rightarrow (BBA)_3$-$^1ZnP^*$-$CO_2H$, with the efficiencies of 28-68%. The comparison of the first oxidation potential and $E_{0\text{-}0}$ of BBA and the first reduction potential of ZnP revealed the possibility of photo-induced electron transfer (PET) from the $^1BBA^*$ to ZnP, in addition to the PEnT, and the component was calculated to be 27-70%. The density functional theory (DFT) studies have shown that, in these tetrads, HOMO is mainly concentrated on BBA moieties while LUMO on the porphyrin macrocycle and the carboxylic acid functional group indicating that, once anchored onto TiO_2 nanoparticles, these tetrads can be utilized as the sensitizers for DSSCs.

Keywords. Bis(4′-*tert*-butylbiphenyl-4-yl)aniline; photo-induced electron transfer; photo-induced energy transfer.

1. Introduction

In photosynthesis, light-harvesting systems enclosed in the chloroplast funnel the incident photons to the reaction center very efficiently.[1] In this system co-facially oriented, slip-stacked chlorophyll and bacteriochlorophyll molecules are densely packed and promote easy and quick inter-ring energy transfer. During the last few decades, chemists are inspired by these complexes and have designed various porphyrin-based donor-acceptor architectures by using concepts of both covalent and non-covalent interactions.[2–4] In electron and energy donor-acceptor (D-A) systems, understanding the charge-transfer processes, producing a long-lived charge-separated (CS) state, as well as achieving a longer lifetime for the charge recombination (CR) state is crucial to achieving goals in the field of photovoltaics and light-emitting diodes.[5–9]

*For correspondence

Supplementary Information: The online version contains supplementary material available at https://doi.org/10.1007/s12039-021-01958-7.

Published online: 09 September 2021

Donor-acceptor systems with a basic model of secondary donor–primary donor-acceptor (D_2-D_1-A) usually exhibit sequential electron transfer. In these systems, the chromophores are usually covalently linked or connected *via* self-assembled approaches.[10–16] Generally in these models, when the primary electron donor is selectively excited, an ET takes place from D_1^* to A creating a cation radical on D_1 ($D_1^{+\cdot}$) and an anion radical on A ($A^{-\cdot}$). Sequentially, a hole is shifted from D_2 to $D_1^{+\cdot}$ to create a long-lasting CS state ($D_2^{+\cdot}$-D_1-$A^{-\cdot}$) with significant lifetimes. In this direction of creating such donor-acceptor models, very well established and studied chromophores such as porphyrins and fullerenes have been employed as molecular building blocks because of their optical, electron-rich, photochemical and electrochemical properties.[11–21] Fullerenes (C_{60} and C_{70}) are used as acceptors in these donor-acceptor models because of their low re-organization energy. In the electron transfer reactions, fullerene exhibits small re-organization that speeds up the forward electron transfer (k_{cs}) and slows down the back electron transfer process (k_{CR}).[10,22–25] As terminal secondary electron donors, triphenylamine,[15] phenothiazine,[16] ferrocene[21,26–32] tetrathiofulvalene,[33–38] etc. have been employed.

Triphenylamine (TPA) compounds have been developed as interesting precursors of small molecule-based materials for application in photo organic materials.[39–41] These molecules possess low oxidation potential values, due to which they behave as attractive hole transporting materials in various fields like organic light-emitting diodes,[42–44] and organic solar cells.[45–47] In *N,N*-dialkyl derivatives, a twisted geometry exists around the nitrogen atom which decreases the π-donor strength of the amino group through orbital coupling[48,49] and hence, the π-π aggregation is prevented and affects the fluorescence properties in the solid state.[50–52] Among a wide variety of donor molecules *N, N*-bis(4′-*tert*-butylbiphenyl-4-yl)aniline), abbreviated as BBA, is one of the strong electron donors because BBA forms stable amine radical cation similar to dimethylaniline and triphenylamines.

On the other hand, porphyrins are the most attractive species because of their structural similarity with chlorophylls, and participate in photon capture in the electron transfer cascades similar to that in natural photosynthesis.[17,53,54] Porphyrins show unique optical and redox properties which can be tuned by functionalizing different groups on the porphyrin core or *via* non-covalent interactions with the metal ions placed in the core of porphyrin.[6,55] Similarly, push-pull porphyrins have emerged as potential molecules in dye-sensitized solar cells (DSSC) and non-linear optics.[56,57] These chromophores have been effectively used as the donors in ET/EnT cascades of the design D-π-A in which D and A are separated by a π-spacer. The tunability of the HOMO-LUMO gap can modify their intra and intermolecular charge transactions, like CS and CR properties.[58]

In literature, very few examples have been reported regarding the triarylamine-porphyrin hybrids.[59–61] The optical and redox properties of these porphyrin cores were tuned meaningfully by substituting the meso-positions by TPA moieties. TPA-porphyrin-fullerene (C_{60}) was reported as a $(donor)_2$-$(donor)_1$-acceptor multimodular hybrid, and this system demonstrated sequential EnT followed by ET efficiently, where EnT takes place from the $^1TPA^*$ to ZnP followed by ET from $^1ZnP^*$ to the C_{60}. In addition, the TPA substituents were involved in stabilizing the cation radical of ZnP as well as anion radical of C_{60}, ZnP^+-$C_{60}^{-\cdot}$, in a CS state by a charge-dissipation mechanism.[62] The CS state ultimate lifetime was as long as 1 μs.[63] Among the family of triphenylamines, BBA, emerged as a strong electron donor that has the intriguing ability to stabilize the charge-separated and exhibits the cation radical at 745 and 900 nm.[64] Few studies involving the BBA-fullerene dyads and PCT and CR dynamics upon excitation of the fullerene have been reported.[65–71] In literature, our group discussed systematic femtosecond time-resolved fluorescence and transient absorption studies in three covalently linked BBA-fullerene dyads involving the excitation dependent electron exchange energy transfer from $^1BBA^* \rightarrow C_{60}$ followed by an ET from BBA $\rightarrow$ $^1C_{60}^*$ leading to the construction of the CS state, $BBA^{+\cdot}$-$C_{60}^{-\cdot}$ [64] in polar solvents. Also, BBA-functionalized boron-dipyrromethenes with varied spacer sizes were synthesized by us and the excitation wavelength-dependent PET and twisted intramolecular charge transfer (TICT) were reported.[72] We have also synthesized BBA-substituted A_3B zinc porphyrin as light harvesting material for DSSC for conversion of light energy to electricity and a power conversion efficiency of 3.8% was reported.[73] Encouraged by these results, we have designed and synthesized three BBA-porphyrin tetards, **Tetrads 1-3,** containing three BBA moieties connected to the three meso-positions of the porphyrin macrocycle *via* three different spacers, i.e., directly connected, phenyl and ethoxy phenyl, and a carboxylic acid functional group at the other meso-position and structural integrity was fully characterized using ^1H, ^{13}C NMR and mass spectrometric studies. The photophysical properties of these tetrads

were studied using UV-visible and steady state fluorescence studies. Computational studies were performed to visualize optimized geometries and identify the sites of electron relay and, thereby, obtain the information whether the tetrads possess the promising potential to behave as the sensitizers for DSSC applications (Figure 1).

2. Experimental

2.1 *Materials and physical measurements*

The chemicals and reagents used for the synthesis of the tetrads and control compounds were purchased from commercial suppliers. The reactions were performed in distilled solvents under inert atmosphere whenever needed, and the crude compounds were purified by laboratory reagent grade solvents. The spectroscopic investigations were performed in spectroscopic grade solvents procured from Sigma-Aldrich. Thin layer chromatography was used to check the progress of the reaction and the purity of the compounds.

^{1}H-NMR spectra were recorded on a 500 MHz Bruker Advances spectrometer. Cary 100 UV/Vis spectrophotometer (UV1106M034) procured from Agilent Technologies was used to record the absorption spectra of the compounds while fluorescence spectrometer (LS55) purchased from Perkin Elmer was used to record the emission spectra of all the compounds. In both the cases 1.0 cm quartz cells were used.

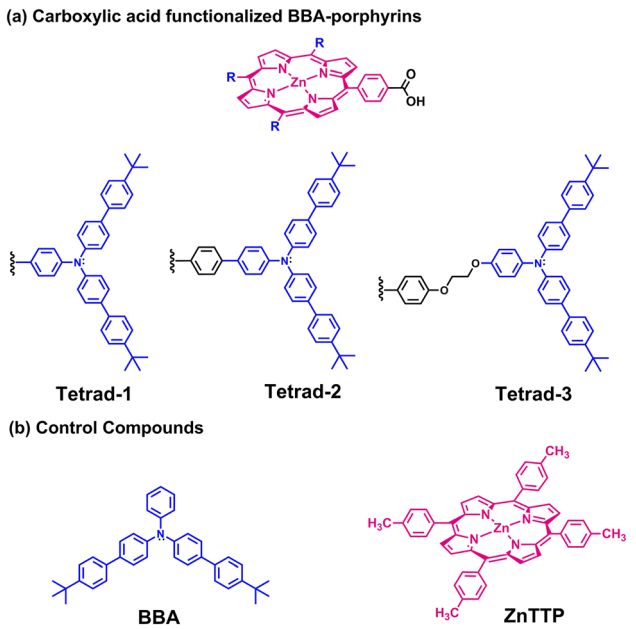

Figure 1. Structures of the carboxylic acid functionalized *N, N*-bis(4′-*tert*-butylbiphenyl-4-yl)aniline) substituted porphyrin compounds employed for the study.

2.2 *Theoretical measurements*

The geometries of the tetrads were optimized using Grimis-Geometry, Frequency, Noncovalent, eXtended Tight Binding (GFN-xTB) theory[74] and the same level of theory was used to calculate frequencies. Energy convergence criteria was set to 10^{-10} eV during geometry optimization and frequency calculations. All these calculations were carried out using SCM-DFTB simulation package.[75] The GFN-xTB optimized geometries were used to probe the single point calculations. The results reported herein are obtained using DFT based Becke's three parameter hybrid exchange functional and Lee-Yang-Parr correlation functional (B3LYP) employing 6-31G* basis set. These calculations were performed using Gaussian 16 suite program.[76]

2.3 *Synthesis details*

N, N-bis(4′-*tert*-butylbiphenyl-4-yl)aniline) (**BBA**) (**1**), *N,* *N*-bis(4′-*tert*-butylbiphenyl-4-yl)4-bromoaniline (**BBA-Br**) (**2**), 4-(Bis(4′-*tert*-butylbiphenyl-4-yl)amino)benzaldehyde (**3**), 4′-(Bis(4′-*tert*-butylbiphenyl-4-yl)amino)biphenyl-4-carbaldehyde (**4**), were synthesized by the literature procedures reported earlier.[64] The synthetic details of the compounds **1**, **2**, **3**, and **4** along with the ^{1}H and ^{13}C NMR (Figures S1-S8, SI) and mass spectra (Figures S24-S27, SI) are provided in the supporting information.

2.3a *Synthesis of Bis(4′-tert-butylbiphenyl-4-yl) anisidine) (BBA-OMe) (5)*: To a schlenk flask was added 4-bromo-4-*tert*-butylbiphenyl (2 g, 6.91 mmol), Na^{t}Bu (828 mg, 8.62 mmol), $Pd(dba)_2$ (18.88 mg, 0.03 mmol), dppf (27.15 mg, 0.04 mmol), and dry toluene (40 mL) under inert atmosphere. Then added *p*-anisidine (322 mg 3.45 mmol) and refluxed reaction mixture for 14 h. After completion of the reaction, the reaction mixture was poured into water and extracted with diethyl ether. The organic layer was dried over sodium sulphate. Compound was isolated on a silica gel column chromatography using hexane: toluene (70:30 v/v) as an eluent. Yield 79%. ^{1}H NMR ($CDCl_3$, 500 Hz): δ 7.50 (d, J = 8 Hz, 12H, phenyl-*H*), 7.15-7.11 (m, 6H, phenyl-*H*), 6.87 (d, J = 9 Hz, 2H, phenyl-*H*), 3.81 (s, 3H, -OCH_3), 1.36 (s, 18H, *tert*-butyl-*H*). ^{13}C NMR ($CDCl_3$, 125 Hz): 31.41, 34.52, 55.53, 114.86, 122.94, 125.69, 126.29, 127.58, 134.47,

137.89, 140.52, 147.08, 149.68, 156.37, 55.06. HRMS (ESI+) (m/z): $[M+K]^+$ calculated for $C_{39}H_{41}NOK$ 578.2825; found 578.2820.

2.3b *4-(bis(4′-tert-butylbiphenyl-4-yl)amino)phenol (BBA-OH) (6)*: In a two-necked round-bottomed flask was placed **5** (1.2 g, 2.23 mmol) in anhydrous $CHCl_3$ (30 mL). A solution of 1M boron tribromide (3 mL, 3.00 mmol) was added dropwise at –78 °C, and the mixture was stirred at room temperature for 3 h. The mixture was poured onto ice and extracted with $CHCl_3$ (330 mL). The organic layers were dried over anhydrous sodium sulfate, filtered, and concentrated under reduced pressure. The crude product was purified by silica gel column chromatography using petroleum ether:toluene (10:90 v/v) as an eluent. Evaporation of the solvent yielded the titled compound as solid. Yield: 70%. HRMS (ESI+) (m/z): $[M+H]^+$ calculated for $C_{38}H_{40}NO$ requires 526.3110; found 526.3104..

2.3c *4-bis (4′-tert-butylbiphenyl-4-yl) amino)phenylethoxybenzaldehyde (7)*: To a solution of **6** (2 g, 3.80 mmol) dissolved in DMF (30 mL) was added K2CO3 (2.63 g, 51.32 mmol). To the resulting mixture was added bromoethoxybenzaldehyde (2 g, 9.51 mmol) at 80 °C and refluxed for 18 h. The reaction mixture was washed with water, extracted by using ethyl acetate, and dried over sodium sulphate. The compound was purified over silica gel using petroleum ether/toluene (30:70 v/v) as eluent. Yield 1.8 g (49%). ^{1}H NMR ($CDCl_3$, 500 Hz): δ 9.90 (s, 1H,-CHO), 7.86 (d, *J* = 9 Hz, 2H, phenyl-*H*), 7.51 (d, *J* = 8.5 Hz, 4H, phenyl-*H*), 7.45 (t, *J* = 8.5 Hz, 8H, phenyl-*H*), 7.17 (d, *J* = 9 Hz, 2H, phenyl-*H*), 7.12 (d, *J* = 8.5 Hz, 4H, phenyl-*H*), 7.07 (d, *J* = 8.5 Hz, 2H, phenyl-*H*), 6.92 (d, *J* = 9 Hz, 2H, phenyl-*H*), 4.397 (dd, *J*=9.5 Hz, 4H, -O-CH_2-CH_2-O), 1.36 (s, 18H, *tert*-butyl-*H*). ^{13}C NMR ($CDCl_3$, 125 Hz): 31.41, 34.53, 66.56, 66.87, 114.95, 115.65, 123.10, 125.71, 126.29, 127.40, 127.62, 130.28, 132.05, 134.65, 137.82, 141.19, 146.99, 149.75, 155.06, 163.66, 190.84.

2.3d *General procedure for the synthesis of A_3B-ester porphyrins*: In a two neck round-bottomed flask aldehyde (3 eq.) and methyl 4-formylbenzoate (1 eq.) were dissolved in propionic acid (45 mL), acetic acid (45 mL), and nitrobenzene (15 mL) and the reaction mixture was heated to reflux at 140 °C. Then pyrrole (4 eq) was added slowly to the reaction mixture and the system was kept at reflux for 12 h. After aldehyde was consumed completely, the reaction mixture was cooled to room temperature and the solvents were removed by vacuum distillation. The residue was dissolved in dichloromethane (50 mL), poured into 40 mL ammonia solution and stirred overnight. The crude compound was extracted using dichloromethane and the organic extracts were evaporated under reduced pressure. The crude compound was purified by basic alumina column chromatography using petroleum ether/toluene (20:80 v/v) as an eluent. Evaporation of the solvent yielded the titled compound as a purple solid. Yield: ∼ 6%.

2.3e *5-(4-methoxycarbonylphenyl)10,15,20-tris(4-(Bis(4′-tert-butylbiphenyl-4-yl)aminophenyl) porphyrin (8)*: ^{1}H NMR ($CDCl_3$, 500 Hz): δ 9.10 (s, 6H, pyrrole-*H*), 8.81 (d, *J* = 4.5 Hz, 2H, pyrrole-*H*), 8.46 (d, *J* = 8 Hz, 2H, phenyl-*H*), 8.33 (d, *J* = 8 Hz, 2H, phenyl-*H*), 8.13 (t, *J* = 9 Hz, 6H, phenyl-*H*), 7.66-7.65 (m, 12H, phenyl-*H*), 7.64-7.59 (m, 12H, phenyl-*H*), 7.57-7.51 (m, 6H, phenyl-*H*), 7.50-7.48 (m, 24H, phenyl-*H*), 4.31 (s, 3H, -OMe), 1.38 (s, 54H, *tert*-butyl-*H*), -2.65 (s, 2H, imino-*H*).

2.3f *5-(4-methoxycarbonylphenyl)10,15,20-tris(4-(Bis(4′-tert-butylbiphenyl-4-yl) aminobiphenyl)porphyrin (9)*: ^{1}H NMR ($CDCl_3$, 500 Hz): δ 8.96 (s, 6H, pyrrole-*H*), 8.81 (s, 2H, pyrrole-*H*), 8.45 (d, *J* = 6.5 Hz, 2H, phenyl-*H*), 8.33-8.24 (m, 8H, phenyl-*H*), 7.99-7.92 (m, 8H, phenyl-*H*), 7.80 (s, 6H, phenyl-*H*), 7.61-7.56 (m, 24H, phenyl-*H*), 7.48 (d, *J* = 7.5 Hz, 12H, phenyl-*H*), 7.50 (d, *J* = 6.5 Hz, 6H, phenyl-*H*), 7.30 (d, *J* = 7.5 Hz, 10H, phenyl-*H*), 4.12 (s, 3H, -OMe), 1.39 (s, 54H, *tert*-butyl-*H*), -2.68 (s, 2H, imino-*H*).

2.3g *5-(4-methoxycarbonylphenyl)10,15,20-tris(4-(Bis(4′-tert-butylbiphenyl-4-yl) aminophenylethoxyphenyl)porphyrin (10)*: ^{1}H NMR ($CDCl_3$, 500 Hz): δ 8.89 (s, 6H, pyrrole-*H*), 8.79 (d, *J* = 5 Hz, 2H, pyrrole-*H*), 8.44 (d, *J* = 8 Hz, 2H, phenyl-*H*), 8.30 (d, *J* = 8 Hz, 2H, phenyl-*H*), 8.14 (d, *J* = 8 Hz, 6H, phenyl-*H*), 7.52-7.48 (m, 24H, phenyl-*H*), 7.44 (d, *J* = 10 Hz, 12H, phenyl-*H*), 7.36-7.34 (m, 6H, phenyl-*H*), 7.24 (d, *J* = 8.5 Hz, 6H, phenyl-*H*), 7.17 (d, *J* = 8.5 Hz, 12H, phenyl-*H*), 7.06 (d, *J* = 8.5Hz, 6H, phenyl-*H*), 4.63 (d, *J* = 4.5Hz, 6H, OCH_2CH_2), 4.53 (d, *J* = 4.8 Hz, 6H, CH_2CH_2O), 4.11 (s, 3H, -OMe), 1.36 (s, 54H, *tert*-butyl-*H*), -2.74 (s,2H, imino-*H*).

2.3h *Hydrolysis of the ester functionalized porphyrins*: The respective ester functionalized

porphyrin (**8** or **9** or **10**) (120 mg) was dissolved in 40 mL solvent (THF: MeOH: 3:1 (v/v)), added 20 equivalents of 1M aqueous KOH to the solution and refluxed for 10h. After cooling to room temperature, the reaction mixture was treated slowly with 0.1 M HCl, washed with $NaHCO_3$ and extracted using chloroform. The organic layers were dried over sodium sulphate and the solvent was evaporated under reduced pressure. The crude compound was purified by using column chromatography.

2.3i *5-(4-carboxylphenyl)10,15,20-tris(4-(Bis(4′-tert-butylbiphenyl-4-yl)aminophenyl) porphyrin (11)*: ^{1}H NMR ($CDCl_3$, 500 Hz): δ 9.10 (s, 6H, pyrrole-*H*), 8.84 (d, *J* = 4.5 Hz, 2H, pyrrole-*H*), 8.55 (d, *J* = 7.5 Hz, 2H, phenyl-*H*), 8.39 (d, *J* = 7.5 Hz, 2H, phenyl-*H*), 8.14 (t, *J* = 7.5 Hz, 6H, phenyl-*H*), 7.66-7.61 (m, 12H, phenyl-*H*), 7.59-7.56 (m, 18H, phenyl-*H*), 7.51-7.48 (m, 24H, phenyl-*H*), 1.38 (s, 54H, *tert*-butyl-*H*), -2.63 (s, 2H, imino-*H*).

2.3j *5-(4-carboxylphenyl)10,15,20-tris(4-(Bis(4′-tert-butylbiphenyl-4-yl)aminobiphenyl) porphyrin (12)*: ^{1}H NMR ($CDCl_3$, 500 Hz): δ 8.95-8.87 (m, 8H, pyrrole-*H*), 8.50 (d, *J* = 5.5 Hz, 2H, pyrrole-*H*), 8.30-8.20 (m, 8H, phenyl-*H*), 7.99-7.85 (m, 10H, phenyl-*H*), 7.72 (s, 4H, phenyl-*H*), 7.57-7.47 (m, 34H, phenyl-*H*), 7.39 (d, *J* = 7.5 Hz, 2H, phenyl-*H*), 7.32-7.29 (m, 16H, phenyl-*H*), 1.38 (s, 54H, *tert*-butyl-*H*), -2.66 (s, 2H, imino-*H*).

2.3k *5-(4-carboxylphenyl)10,15,20-tris(4-(Bis(4′-tert-butylbiphenyl-4-yl) aminophenylethoxyphenyl)porphyrin (13)*: ^{1}H NMR ($CDCl_3$, 500 Hz): δ 8.90 (s, 6H, pyrrole-*H*), 8.82 (d, *J* = 3 Hz, 2H, pyrrole-*H*), 8.54 (d, *J* = 7.5 Hz, 2H, phenyl-*H*), 8.36 (d, *J* = 7.5 Hz, 2H, phenyl-*H*), 8.12 (s, 6H, phenyl-*H*), 7.53-7.48 (m, 24H, phenyl-*H*), 7.45 – 7.43 (m, 12H, phenyl-*H*), 7.31(s, 6H, phenyl-*H*), 7.23 (d, *J* = 8.5 Hz, 6H, phenyl-*H*), 7.17 (d, *J* = 8.5 Hz, 12H, phenyl-*H*), 7.05- 7.03 (m, 6H, phenyl-*H*), 4.56 (s, 6H, -OCH_2CH_2O), 4.48 (s, 6H, OCH_2CH_2O), 1.36(s, 54H,-*tert*-butyl-*H*), -2.70 (s, 2H, imino-*H*).

2.3l *Zinc metalation of the carboxylic acid functionalized free base porphyrins*: The respective carboxylic acid functionalized free base porphyrin (**11** or **12** or **13**) (80 mg) was dissolved in 30 mL chloroform. To this reaction mixture saturated $Zn(CH_3COO)_2.2H_2O$ solution in methanol (5 mL) was added and the reaction mixture was refluxed for 1h. Reaction progress was monitored using UV–visible spectroscopy. Once the reaction is complete, the solution was concentrated under reduced pressure and purified over silica gel column using chloroform as eluent to yield the zinc porphyrins (**14** or **15** or **16**).

2.3m *5-(4-carboxylphenyl)10,15,20-tris(4-(Bis(4′-tert-butylbiphenyl-4-yl)aminophenyl) porphyrinatozinc(II) (14)*: ^{1}H NMR ($CDCl_3$, 500 Hz): δ 9.15 (s, 6H,-pyrrole-*H*), 8.94 (d, *J* = 4.5 Hz, 2H, pyrrole-*H*), 8.52 (d, *J* = 8 Hz, 2H, phenyl-*H*), 8.38 (d, *J* = 7.5 Hz, 2H, phenyl-*H*), 8.14 (s, 6H, phenyl-*H*), 7.66-7.60 (m, 12H, phenyl-*H*), 7.59-7.52 (m, 18H, phenyl-*H*), 7.50-7.48 (m, 24H, phenyl-*H*), 1.38 (s, 54H, *tert*-butyl-*H*).

2.3n *5-(4-carboxylphenyl)10,15,20-tris(4-(Bis(4′-tert-butylbiphenyl-4-yl)aminobiphenyl) porphyrinatozinc(II): (15)*: ^{1}H NMR ($CDCl_3$, 500 Hz): δ 9.08 (s, 6H, pyrrole-*H*), 8.93 (s, 2H, pyrrole-*H*), 8.46 (s, 2H, pyrrole-*H*),8.30 (s, 8H, phenyl-*H*), 8.02-7.95 (m, 10H, phenyl-*H*), 7.88 (d, 4H, *J* = 10 Hz, phenyl-*H*), 7.59-7.32 (m, 52H, phenyl-*H*), 1.38 (s, 54H, *tert*-butyl-*H*).

2.3o *5-(4-carboxylphenyl)10,15,20-tris(4-(Bis(4′-tert-butylbiphenyl-4-yl) aminophenylethoxyphenyl) porphyrinatozinc (II) (16)*: ^{1}H NMR ($CDCl_3$, 500 Hz): δ 9.00 (s, 6H, pyrrole-*H*), 8.91 (d, *J* = 8.5 Hz, 2H, pyrrole-*H*), 8.50 (d, *J* = 7.5 Hz, 2H, phenyl-*H*), 8.35 (d, *J* = 8 Hz, 2H, phenyl-*H*), 8.14 (d, *J* = 8 Hz, 6H, phenyl-*H*), 7.52-7.47 (m, 24H, phenyl-*H*), 7.44–7.42 (m, 12H, phenyl-*H*), 7.33 (d, *J* = 7.5 Hz, 6H, phenyl-*H*), 7.23 (d, *J* = 8.5 Hz, 6H, phenyl-*H*), 7.17 (d, *J* = 8.5 Hz, 12H, phenyl-*H*), 7.04 (d, *J* = 8 Hz, 6H, phenyl-*H*), 4.61 (s, 6H, OCH_2CH_2O), 4.51 (s, 6H, OCH_2CH_2O), 1.36 (s, 54H, *tert*-butyl-*H*).

3. Results and Discussion

3.1 *Synthesis of N, N-bis (4′-tert-butylbiphenyl-4-yl)aniline) substituted porphyrin derivatives*

The synthesis of the BBA functionalized porphyrin tetrads, **Tetrad-1, Tetrad-2,** and **Tetrad-3** employed for the present study is outlined in Scheme 1. Initially, the synthesis of **1 (BBA)** was achieved by reacting 4-bromo-4-*tert*-butylbiphenyl with aniline in the presence of $Pd(dba)_2$ catalyst, followed by bromination using NBS to yield **2 (BBA-Br)**. Formylation of **1** using DMF and $POCl_3$ under standard Vilsmeier-Haack reaction conditions yielded **3 (R_1-CHO)** while

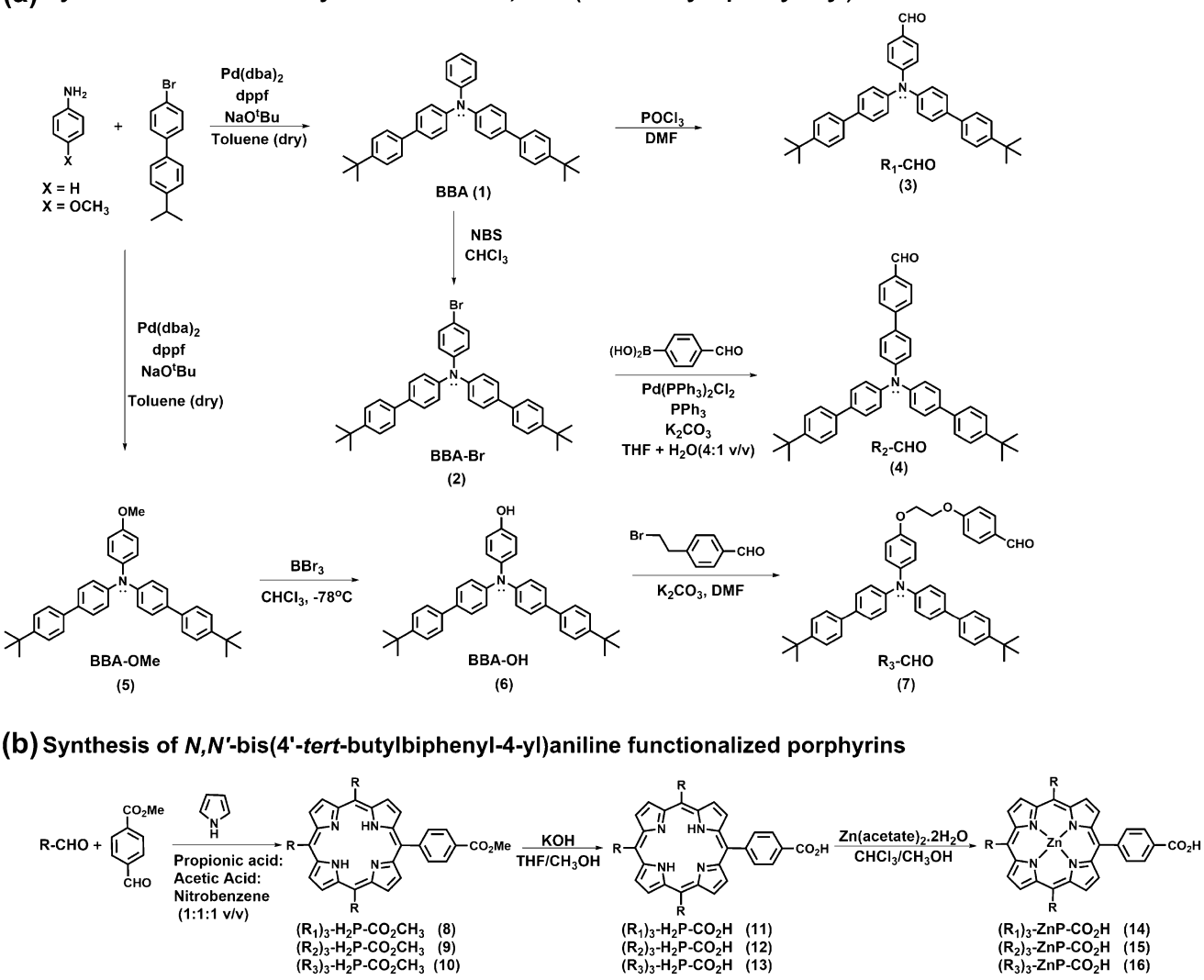

Scheme 1. Synthetic scheme of carboxylic acid substituted BBA-zinc porphyrins.

4 (**R_2-CHO**) was obtained by reacting 4-formylphenylboronic acid in the presence of Pd catalyst under Suzuki coupling conditions. The synthesis of **5** (**BBA-OCH_3**) was achieved by reacting 4-bromo-4-*tert*-butylbiphenyl with *p*-anisidine in the presence of $Pd(dba)_2$ catalyst. Demethylation of **5** using BBr_3 yielded **6**, which upon subsequent nucleophilic substitution reaction with bromoethoxy benzaldehyde in the presence of K_2CO_3 in DMF yielded **7** (**R_3-CHO**).

For the synthesis of porphyrins, the aldehyde precursors, **3** or **4** or **7** were mixed with methyl 4-formylbenzoate and pyrrole in a solvent mixture of propionic acid, acetic acid, and nitrobenzene and were refluxed at 140 °C. Purification of the ester functionalized porphyrins followed by hydrolysis in the presence of KOH in THF/CH_3OH yielded the acid derivatives. Furthermore, metalation of the carboxylic acid functionalized free base porphyrins using zinc acetate in methanol yielded the BBA-substituted porphyrins, **Tetrad-1, Tetrad-2,** and **Tetrad-3** in good yields. All BBA-porphyrin tetrads were soluble in $CHCl_3$ and CH_2Cl_2 which allowed us to perform the systematic photophysical studies with greater ease.

3.2 *Optical absorption studies*

The absorption spectra of BBA- porphyrin tetrads, **Tetrad-1, Tetrad-2,** and **Tetrad-3**, along with reference compounds, **BBA** and 5,10,15,20-tetratolylporphyrinatozinc(II) (**ZnTTP**) were recorded in 1,2-DCB (Figure 2).

The control compounds, **BBA** exhibited a peak around 343 nm whereas **ZnTTP** at 426 nm (soret) and

553 and 597 nm (Q-bands). **Tetrad-1** displayed absorption bands at 345, 442, 559, and 604 nm and were observed to be red-shifted (vs **BBA**: ~ 2 nm) and (vs **ZnTTP**: ~27 nm) indicating strong interactions among the chromophores in the ground state and the absence of aggregates due to the strategic selection of non-planar BBA moieties. In case of **Tetrad-2**, the absorption due to BBA moiety (λ_{max}: 352 nm) was red-shifted by 7 nm compared to control compound, **BBA** whereas the porphyrin peaks were shifted by 2-5 nm. This bathochromic shift can be mainly attributed to the increase in conjugation due to the introduction of the phenyl spacers between chromophores. The absorption spectrum of the **Tetrad-3** looked like the combination of the absorption spectra of **BBA** and **ZnTTP** with very marginal shifts (~ 2 nm) indicating that the presence of the ethyloxy spacer did not provide any kind of major electronic communication between the chromophores in the ground state.

More importantly, in these tetrads, the BBA moiety absorption at 335 nm had no overlap with the absorption of zinc porphyrin at this wavelength indicating that the photo-excitation at this particular wavelength would lead to selective excitation of BBA moiety in the tetrads.

3.3 *Steady state fluorescence studies*

Figure S30, SI shows the spectral overlap of the emission of the **BBA** with the absorption of the **ZnTTP**, indicating that in **Tetrads 1-3**, selective excitation of the BBA moiety would lead to a PEnT from ^{1}BBA* to **ZnTTP** moiety generating excited ZnP. In order to explore this, the fluorescence spectra of the tetrads and the control compounds were recorded in 1,2-DCB (Figure 3).

Upon excitation of the equi-absorbing solutions of BBA-ZnP tetrads, **Tetrads 1-3**, and the control compounds, **BBA** and **ZnTTP** at 352 nm, the wavelength at which the BBA moiety is excited predominantly, in 1,2-DCB, the emission corresponding to the BBA moiety, was observed at 395 nm only in case of **BBA**. Whereas in case of the tetrads, the emission of the **BBA** moiety was quenched with the appearance of the porphyrin emission at 618 nm (**Tetrad-1**) or 605 nm (**Tetrad-2** & **Tetrad-3**) indicating the occurrence of PEnT from ^{1}BTZ* to ZnP in these systems. It should be noted here that excitation of equi-absorbing solution of **ZnTTP** at this wavelength did not show any noticeable porphyrin emission bands in the range of 590-650 nm indicating that the excitation of these tetrads at 370 nm excited the BBA moiety predominantly. Similar results displaying photo-induced energy transfer from ^{1}BBA* to ZnP moiety was observed by our research group earlier in case of the $(BBA)_4$-ZnP compounds when the BBA was excited selectively at 335 nm.[77] Also, it should be mentioned here that, to the best of our knowledge, the synthesis of the carboxylic acid appended porphyrins and photo-excitation of the BBA leading to the PEnT from singlet excited BTZ to ZnP is not reported till date.

The excitation spectra of the tetrads were recorded by monitoring the emission of the ZnP at 618 nm for **Tetrad-1** or 605 nm for both **Tetrad-2** & **Tetrad-3**. The spectra thus obtained appeared to be similar to the absorption spectra of the tetrads (see Figure S31, SI), providing the evidence of intramolecular PEnT in these tetrads. The efficiencies of PEnT in these tetrads were estimated by integrating and comparing the area

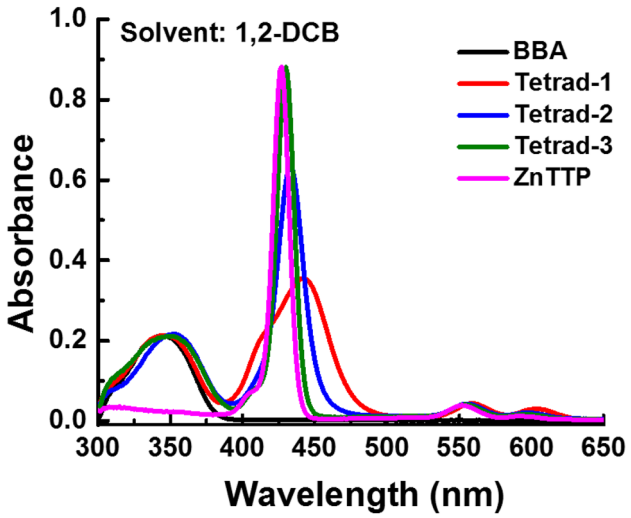

Figure 2. Absorption spectra of the specified compounds in 1,2-DCB.

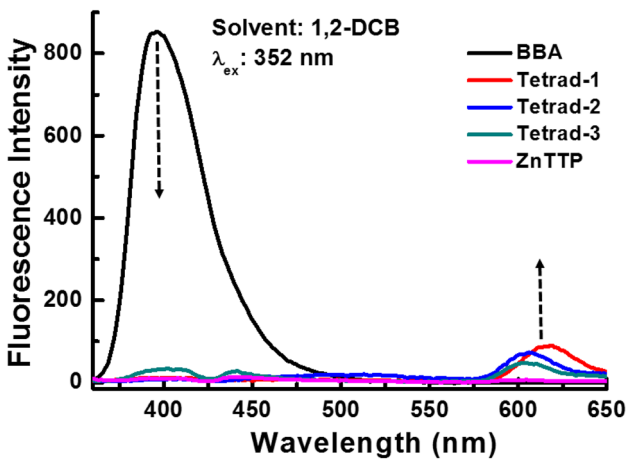

Figure 3. Emission spectra (λ_{ex} = 352 nm) and (OD λ_{abs} = 0.1) of equiabsorbing compositions of **BBA, ZnTTP** and **Tetrad-1, Tetrad-2,** and **Tetrad-3** in 1,2-DCB.

under the BBA peak in the absorption and excitation spectra and were calculated to be 28%, 53%, and 68% in case of **Tetrad-1, Tetrad-2,** and **Tetrad-3** in 1,2-DCB respectively.

Among various radiative and non-radiative intramolecular processes that decay the excited state of the chromophores of the tetrads, in addition to PEnT, PET can be conceived as one of the photophysical pathways for quenching the fluorescence intensity. The efficiency of the fluorescence quenching, %Q, was estimated by integrating and comparing the area under the BBA moiety emission peak in the control compound, **BBA**, and the tetrads and were calculated to be 98%, 97%, and 95% in case of **Tetrad-1**, **Tetrad-2**, and **Tetrad-3** in 1,2-DCB respectively. A literature survey of the first oxidation potential[72] (0.87 V vs SCE) and $E_{0\text{-}0}$ (3.4 eV) of the BBA and the first reduction potential of the **ZnTTP**[78] (-1.44 vs SCE) indicates a possibility of PET from $^{1}BBA^{*}$ to ZnP in these tetrads. The possible PET component in the tetrads was estimated by taking the difference between the %Q and %PEnT and was calculated to be 70%, 44%, and 27% in the case of **Tetrad-1**, **Tetrad-2**, and **Tetrad-3** in 1,2-DCB, respectively.

3.4 *Computational studies*

To probe the electronic structure and properties of the tetrads, the density functional theory (DFT) and tight binding DFT based calculations were performed. As size of systems is significantly large, the geometries were optimized using Grimis-Geometry, Frequency, Noncovalent, eXtended Tight Binding (GFN-xTB) theory.[74] The same level of theory was used to calculate frequencies. All the geometries were found to be the minimum energy structures on corresponding potential energy surfaces by frequency analysis. Energy convergence criteria was set to 10^{-10} eV during geometry optimization and frequency calculations. All these calculations were carried out using SCM-DFTB simulation package.[75]

The GFN-xTB optimized geometries were used to probe the single-point calculations. The results reported herein are obtained using DFT based Becke's three parameter hybrid exchange functional and Lee-Yang-Parr correlation functional (B3LYP) employing 6-31G* basis set. These calculations were performed using Gaussian 16 suite program.[76]

It is interesting to note that the carboxylic anchoring group is perpendicular to the porphyrin ring structure. As **Tetrad-3** possesses more flexible arms the geometry reorganizes significantly. The inclusion of dispersion correction and flexibility of spacer group allow BBA moieties to interact with each other and also with the carboxylic acid group resulting in slanted optimized geometry of **Tetrad-3**. As the spacers between the BBA and ZnP moieties **Tetrad-1** and **Tetrad-2** are relatively rigid and smaller in size, the flexibility of the BBA moieties is limited and allowed them to orient into the fixed planes as shown in Figure 4. The HOMO in **Tetrad-1** and **Tetrad-2** is fully localized on all the BBA moieties while in **Tetrad-3** it is concentrated on a single BBA moiety. On the other hand, LUMOs are fully localized on the porphyrin ring along with the carboxylic acid group (-CO_2H). The HOMO and LUMO energies in **Tetrad-1**, **Tetrad-2**, and **Tetrad-3** are -4.67, -4.71, -4.58 eV and -2.20, -2.22, -2.20 eV, the difference energy gap (E_{LUMO}-E_{HOMO}) are 2.47, 2.49 and 2.38 eV, respectively. We have visualized the HOMO-1, HOMO-2 in **Tetrad-3** and the orbitals are pictorially represented in Figure S32, SI. It can be clearly seen from the figure that the HOMO is situated on single BBA unit in **Tetrad-3**. The HOMO-1 is solely localized on the other BBA unit whose position is directly opposite to that of the carboxylic acid group, while HOMO-2 is mainly concentrated on the other third BBA unit. The DFT calculated energies of HOMO, HOMO-1 and HOMO-2 are -4.58, -4.78, and -4.81 eV, respectively. We have further visualized the positions of LUMO+1 and LUMO+2, we found that the LUMO orbital is located on porphyrin ring as well as the carboxylic acid group. However, LUMO+1 is solely localized on porphyrin ring whereas LUMO+2 is mainly concentrated on carboxylic acid group and a partly also on the porphyrin ring. The energies of LUMO, LUMO+1, and LUMO+2 obtained from DFT studies are -2.20, -2.14, and -1.55 eV. The energy difference between the corresponding HOMO, HOMO-1, and HOMO-2 with the LUMO are 2.38, 2.58, and 2.61 eV, respectively.

In order to explore whether these tetrads can be utilized as the dyes to sensitize the semiconductor TiO_2 nanoparticles, a correlation diagram showing the calculated HOMO-LUMO energy gaps along with the TiO_2 band structure is shown in Figure 5. In the case of all the tetrads, the electron transfer from the LUMO to the conduction band of the TiO_2 appears to be feasible indicating that these tetrads can be used as the sensitizers in DSSCs.

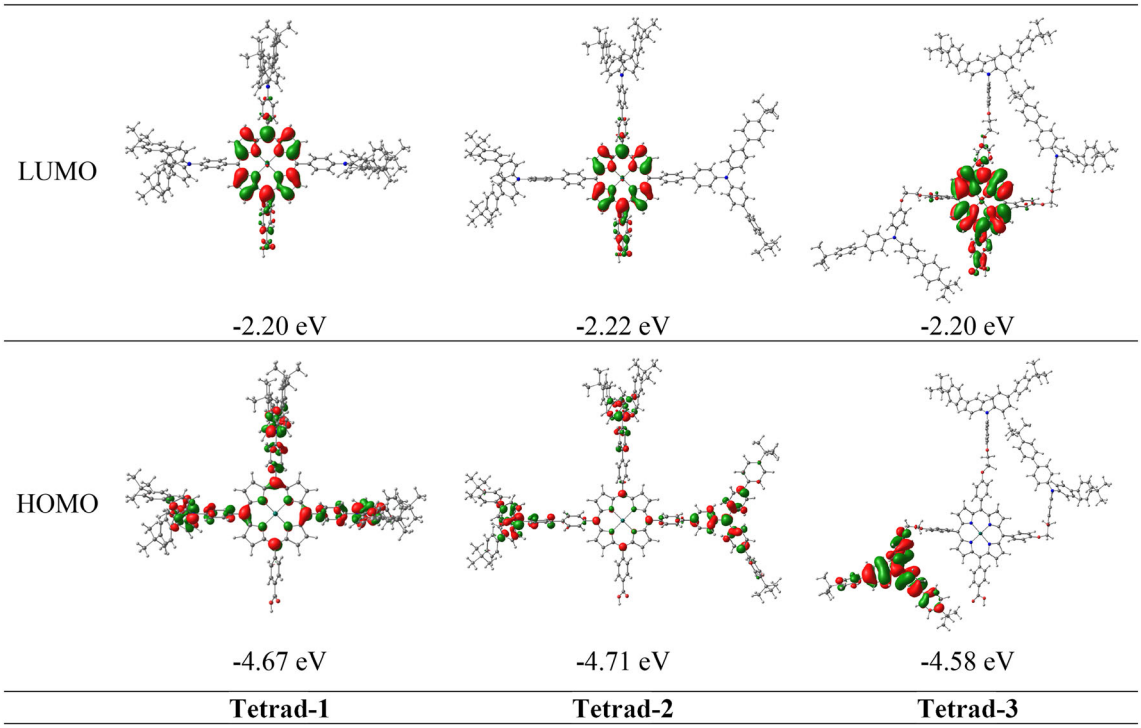

Figure 4. B3LYP/6-31G* calculated frontier HOMO and LUMO orbitals of the tetrads.

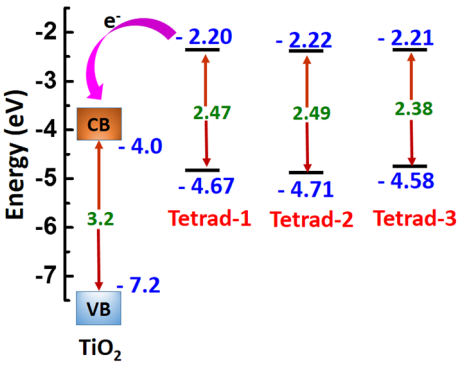

Figure 5. Schematic energy level diagram.

4. Conclusions

A series of BBA functionalized porphyrin tetrads, **Tetrad-1, Tetrad-2,** and **Tetrad-3** containing BBA as a prospective photo-induced energy and electron donor moiety covalently connected to porphyrin macrocycle at meso-positions with varied linker sizes were synthesized and well characterized. When these tetrads were selectively excited at 352 nm, diminished fluorescence intensity of the BBA with a subsequent appearance of the porphyrin emission band at 618 nm was observed signifying the PEnT from ^{1}BBA* to ZnP with the efficiencies of 28-68%. Based on the fluorescence quenching efficiencies, %Q and also the %PEnT, the possible PET component in these tetrads was calculated to be 70-27%. The computational studies have shown that the HOMO is localized mainly on the BBA moieties while the LUMO on the ZnP and carboxylic acid anchoring group indicating that these tetrads can be utilized as the sensitizers in the DSSCs.

Supplementary Information (SI)

Synthesis details of the precursors **1–4**; ^{1}H NMR spectra of the compounds, **1–5**, **7–16**, and ^{13}C NMR spectra of compounds **1–5, 7, 14, 16** (Figures S1–S23); MALDI-TOF of compounds, **1–4** and HRMS (ESI+) of compounds, **5** and **6** (Figures S24–S29); Overlap of the emission spectra of **BBA** and absorption **ZnTTP** in 1,2-DCB (Figure S30); Overlay of the absorption and excitation spectra of (a) **Tetrad-1**, (b) **Tetrad-2**, and (c) **Tetrad-3** 1,2-DCB (Figure S31); Frontier orbitals of **Tetrad-3** and their corresponding energies (Figure S32). Supplementary Information is available at www.ias.ac.in/chemsci.

Acknowledgements

Author RC is grateful to the Department of Science and Technology (DST, CRG/2018/002661), National Institute of Technology Warangal (NITW) for the Research Seed Money (P1078 Plan Gen.-RSM) and also DST-FIST Grants, SR/FST/CSi-257/2014(C) and SR/FST/CSII/2018/65 awarded to Department of Chemistry, Central University

of Rajasthan and Department of Chemistry, NITW respectively, for the financial support of this work. The authors RP is grateful to the Department of Science and Technology (DST, ECR/2018/002346, EEQ/2019/000656). Author SG is grateful to DST and Central University of Rajasthan for the Project fellowship and University fellowship respectively. AB acknowledges DST CRG for the Junior Research Fellowship. Pooja, VRK, and SB acknowledge NITW for the Research Fellowship.

References

1. Mukhopadhyay R D, Kim Y, Koo J and Kim K 2008 Porphyrin boxes *Acc. Chem. Res.* **51** 2730
2. Tanaka T and Osuka A 2015 Conjugated porphyrin arrays: synthesis, properties and applications for functional materials *Chem. Soc. Rev.* **44** 943
3. Bols P S and Anderson H L 2018 Template-directed synthesis of molecular nanorings and cages *Acc. Chem Res.* **51** 2083
4. Li W S and Aida T 2009 Dendrimer porphyrins and phthalocyanines *Chem. Rev.* **109** 6047
5. O'regan B and Grätzel M 1991 A low-cost, high-efficiency solar cell based on dye-sensitized colloidal TiO_2 films *Nature* **353** 737
6. Mathew S, Yella A, Gao P, Humphry-Baker R, Curchod B F, Ashari-Astani N, et al. 2014 Dye-sensitized solar cells with 13% efficiency achieved through the molecular engineering of porphyrin sensitizers *Nat. Chem.* **6** 242
7. Kira A, Umeyama T, Matano Y, Yoshida K, Isoda S, Park J K, et al. 2009 Supramolecular donor−acceptor heterojunctions by vectorial stepwise assembly of porphyrins and coordination-bonded fullerene arrays for photocurrent generation *J. Am. Chem. Soc.* **131** 3198
8. Mohammed O F, Kwon O H, Othon C M and Zewail A H 2009 Charge transfer assisted by collective hydrogen-bonding dynamics *Angew. Chem. Int. Ed.* **48** 6251
9. Deibel C, Strobel T and Dyakonov V 2010 Role of the charge transfer state in organic donor–acceptor solar cells *Adv. Mater.* **22** 4097
10. Sudhakar K, Gokulnath S, Giribabu L, Lim G N, Trâm T and D'Souza F 2015 Ultrafast photoinduced charge separation leading to high-energy radical ion-pairs in directly linked corrole–C60 and triphenylamine–corrole-C60 donor-acceptor conjugates *Chem. Asian J.* **10** 2708
11. Fukuzumi S, Ohkubo K, D'Souza F and Sessler J L 2012 Supramolecular electron transfer by anion binding *Chem. Commun.* **48** 9801
12. D'Souza F and Ito O 2012 In *Multi porphyrin Arrays: Fundamentals and Applications* D Kim (Ed.) (Singapore: Pan Stanford Publishing) **8** 389
13. D'Souza F and Ito O 2012 Photosensitized electron transfer processes of nanocarbons applicable to solar cells *Chem. Soc. Rev.* **41** 86
14. Bottari G, Trukhina O, Ince M and Torres T 2012 Towards artificial photosynthesis: supramolecular, donor–acceptor, porphyrin-and phthalocyanine/carbon nanostructure ensembles *Coord. Chem. Rev.* **256** 2453
15. D'Souza F, Amin A N, El-Khouly M E, Subbaiyan N K, Zandler M E and Fukuzumi S 2012 Control over photoinduced energy and electron transfer in supramolecular polyads of covalently linked azaBODIPY-bisporphyrin 'molecular clip'hosting fullerene *J. Am. Chem. Soc.* **134** 654
16. Chitta R and D'Souza F 2008 Self-assembled tetrapyrrole–fullerene and tetrapyrrole–carbon nanotube donor–acceptor hybrids for light induced electron transfer applications *J. Mater. Chem.* **18** 1440
17. Gust D, Moore A and Moore A L 2009 Solar fuels via artificial photosynthesis *Acc. Chem. Res.* **42** 1890
18. D'Souza F, Chitta R, Gadde S, Shafiqul Islam D M, Schumacher A L, Zandler M E, et al. 2006 Design and studies on supramolecular ferrocene–porphyrin–fullerene constructs for generating long-lived charge separated states *J. Phys. Chem. B* **110** 25240
19. Kodis G, Liddell P A, Moore A L, Moore T A and Gust D 2004 Synthesis and photochemistry of a carotene–porphyrin–fullerene model photosynthetic reaction center *J. Phys. Org. Chem.* **17** 724
20. Imahori H, Sekiguchi Y, Kashiwagi Y, Sato T, Araki Y, Ito O, et al. 2004 Long-lived charge-separated state generated in a ferrocene–meso, meso-linked porphyrin trimer–fullerene pentad with a high quantum yield *Chem. Eur. J.* **10** 3184
21. Imahori H, Tamaki K, Araki Y, Sekiguchi Y, Ito O, Sakata Y and Fukuzumi S 2002 Stepwise charge separation and charge recombination in ferrocene-meso, meso-linked porphyrin dimer–fullerene triad *J. Am. Chem. Soc.* **124** 5165
22. Kirner S V, Guldi D M, Megiatto J D and Schuster D I 2015 Synthesis and photophysical properties of new catenated electron donor–acceptor materials with magnesium and free base porphyrins as donors and C_{60} as the acceptor *Nanoscale* **7** 1145
23. Kawashima Y, Ohkubo K and Fukuzumi S 2013 Small reorganization energies of photoinduced electron transfer between spherical fullerenes *J. Phys. Chem. A* **117** 6737
24. Guldi D M and Asmus K-D 1997 Electron transfer from C76 (C 2 v ') and C78 (D 2) to radical cations of various arenes: evidence for the marcus inverted region *J. Am. Chem. Soc.* **119** 5744
25. Imahori H, El-Khouly M E, Fujitsuka M, Ito O, Sakata Y and Fukuzumi S 2001 Solvent dependence of charge separation and charge recombination rates in porphyrin–fullerene dyad *J. Phys. Chem. A* **105** 325
26. Gokulnath S, Achary B S, Kumar CK, Trivedi R, Sridhar B and Giribabu L 2015 Synthesis, structure and photophysical properties of ferrocenyl or mixed sandwich cobaltocenyl ester linked meso-tetratolylporphyrin dyads *Photochem. Photobiol.* **91** 33
27. Tagliatesta P and Pizzoferrato R 2015 Synthesis and characterization of new ferrocene, porphyrin and C_{60} triads, connected by triple bonds *J. Organomet. Chem.* **787** 27
28. Melomedov J, Ochsmann J R, Meister M, Laquai F and Heinze K 2014 Aminoferrocene and ferrocene amino acid as electron donors in modular porphyrin-ferrocene and porphyrin–ferrocene–porphyrin conjugates *Eur. J. Inorg. Chem.* **20** 2902

29. Pareek Y, Lakshmi V and Ravikanth M 2014 Axially bonded pentads constructed on the Sn (IV) porphyrin scaffold *Dalton Trans.* **43** 6870
30. Lee S-H, Larsen A G, Ohkubo K, Cai Z-L, Reimers J R, Fukuzumi S and Crossley M J 2012 Long-lived long-distance photochemically induced spin-polarized charge separation in β, β′-pyrrolic fused ferrocene-porphyrin-fullerene systems *Chem. Sci.* **3** 257
31. Xenogiannopoulou E, Medved M, Iliopoulos K, Couris S, Papadopoulos M G, Bonifazi D, et al. 2007 Nonlinear optical properties of ferrocene-and porphyrin–[60] fullerene dyads *ChemPhysChem* **8** 1056
32. Poddutoori P K, Sandanayaka A S, Hasobe T, Ito O and van der Est A 2010 Photoinduced charge separation in a ferrocene–aluminum (III) porphyrin–fullerene supramolecular triad *J. Phys. Chem. B* **114** 14348
33. Poddutoori P K, Lim G N, Sandanayaka A S, Karr P A, Ito O, D'Souza F, et al. 2015 Axially assembled photosynthetic reaction center mimics composed of tetrathiafulvalene, aluminum (III) porphyrin and fullerene entities *Nanoscale* **7** 12151
34. Poddutoori P K, Bregles L P, Lim G N, Boland P, Kerr R G and D'Souza F 2015 Modulation of energy transfer into sequential electron transfer upon axial coordination of tetrathiafulvalene in an aluminum (III) porphyrin–free-base porphyrin dyad *Inorg. Chem.* **54** 8482
35. Poddutoori P K, Zarrabi N, Moiseev A G, Gumbau-Brisa R, Vassiliev S and van der Est A 2013 Long-lived charge separation in novel axial donor–porphyrin–acceptor triads based on tetrathiafulvalene, aluminum (III) porphyrin and naphthalenediimide *Chem. Eur. J.* **19** 3148
36. Di Valentin M, Bisol A, Agostini G, Liddell P A, Kodis G, Moore A L, et al. 2005 Photoinduced long-lived charge separation in a tetrathiafulvalene–porphyrin–fullerene triad detected by time-resolved electron paramagnetic resonance *J. Phys. Chem. B* **109** 14401
37. Kodis G, Liddell P A, De la Garza L, Moore A L, Moore T A and Gust D 2002 Photoinduced electron transfer in π-extended tetrathiafulvalene–porphyrin–fullerene triad molecules *J. Mater. Chem.* **12** 2100
38. Liddell P A, Kodis G, De La Garza L, Bahr J L, Moore A L, Moore T A and Gust D 2001 Photoinduced electron transfer in tetrathiafulvalene–porphyrin–fullerene molecular triads *Helv. Chim. Acta* **84** 2765
39. Allain C, Schmidt F, Lartia R, Bordeau G, Fiorini-Debuisschert C, Charra F, et al. 2007 Vinyl-pyridinium triphenylamines: novel far-red emitters with high photostability and two-photon absorption properties for staining DNA *ChemBioChem* **8** 424
40. Bordeau G, Lartia R, Metge G, Fiorini-Debuisschert C, Charra F and Teulade-Fichou M-P 2008 Trinaphthylamines as robust organic materials for two-photon-induced fluorescence *J. Am. Chem. Soc.* **130** 16836
41. He G S, Tan L-S, Zheng Q and Prasad P N 2008 Multiphoton absorbing materials: molecular designs, characterizations, and applications *Chem. Rev.* **108** 1245
42. Shirota Y and Kageyama H 2007 Charge carrier transporting molecular materials and their applications in devices *Chem. Rev.* **107** 953
43. Facchetti A 2010 π-conjugated polymers for organic electronics and photovoltaic cell applications *Chem. Mater.* **23** 733
44. He M, Twieg R J, Gubler U, Wright D and Moerner W 2003 Synthesis and photorefractive properties of multifunctional glasses *Chem. Mater.* **15** 1156
45. Kolemen S, Bozdemir O A, Cakmak Y, Barin G, Erten-Ela S, Marszalek M, et al. 2011 Optimization of distyryl-Bodipy chromophores for efficient panchromatic sensitization in dye sensitized solar cells *Chem. Sci.* **2** 949
46. Anémian R, Morel Y, Baldeck P L, Paci B, Kretsch K, Nunzi J-M and Andraud C 2003 Optical limiting in the visible range: molecular engineering around N4, N4′-bis (4-methoxyphenyl)-N4, N4′-diphenyl-4, 4′-diamino-biphenyl *J. Mater. Chem.* **13** 2157
47. Sasabe H and Kido J 2011 Multifunctional materials in high-performance OLEDs: challenges for solid-state lighting *Chem. Mater.* **23** 621
48. Xiao L, Chen Z, Qu B, Luo J, Kong S, Gong Q and Kido J 2011 Recent progresses on materials for electrophosphorescent organic light-emitting devices *Adv. Mater.* **23** 926
49. Yum J-H, Holcombe T W, Kim Y, Rakstys K, Moehl T, Teuscher J, et al. 2003 Blue-coloured highly efficient dye-sensitized solar cells by implementing the diketopyrrolopyrrole chromophore *Sci. Rep.* **3** 2446
50. Kwon O, Barlow S, Odom S A, Beverina L, Thompson N J, Zojer E, et al. 2005 Aromatic amines: a comparison of electron-donor strengths *J. Phys. Chem. A* **109** 9346
51. Ning Z, Chen Z, Zhang Q, Yan Y, Qian S, Cao Y and Tian H 2007 Aggregation-induced emission (AIE)-active starburst triarylamine fluorophores as potential non-doped red emitters for organic light-emitting diodes and Cl2 gas chemodosimeter *Adv. Funct. Mater.* **17** 3799
52. Ishow E, Brosseau A, Clavier G, Nakatani K, Tauc P, Fiorini-Debuisschert C, et al. 2008 A Multicolor emission of small molecule-based amorphous thin films and nanoparticles with a single excitation wavelength *Chem. Mater.* **20** 6597
53. D'Souza F, Smith P M, Zandler M E, McCarty A L, Itou M, Araki Y and Ito O 2004 Energy transfer followed by electron transfer in a supramolecular triad composed of boron dipyrrin, zinc porphyrin, and fullerene: a model for the photosynthetic antenna-reaction center complex *J. Am. Chem. Soc.* **126** 7898
54. D'Souza F and Ito O 2005 otoinduced electron transfer in supramolecular systems of fullerenes functionalized with ligands capable of binding to zinc porphyrins and zinc phthalocyanines *Coord. Chem. Rev.* **249** 1410
55. Senge M O, Fazekas M, Notaras E G, Blau W J, Zawadzka M, Locos O B and Mhuircheartaigh E M 2007 Nonlinear optical properties of porphyrins *Adv. Mater.* **19** 2737
56. Yella A, Lee H-W, Tsao H N, Yi C, Chandiran A K, Nazeeruddin M K, et al. 2011 Porphyrin-sensitized solar cells with cobalt (II/III)–based redox electrolyte exceed 12 percent efficiency *Science* **334** 629
57. Senge M O, Fazekas M, Pintea M, Zawadzka M and Blau W J 2011 5, 15–A2B2-and 5, 15–A2BC-type porphyrins with donor and acceptor groups for use in

nonlinear optics and photodynamic therapy *Eur. J. Org. Chem.* **2011** 5797
58. Yang Y, Solgaard H S and Haider W 2016 Wind, hydro or mixed renewable energy source: preference for electricity products when the share of renewable energy increases *Energy Policy* **97** 521
59. Li B, Xu X, Sun M, Fu Y, Yu G, Liu Y and Bo Z 2002 Porphyrin-cored star polymers as efficient nondoped red light-emitting materials *Macromolecules* **39** 456
60. Clifford J N, Yahioglu G, Milgrom L R and Durrant J R 2002 Molecular control of recombination dynamics in dye sensitized nanocrystalline TiO_2 films *Chem. Commun.* **12** 1260
61. Yen W-N, Lo S-S, Kuo M-C, Mai C-L, Lee G-H, Peng S-M and Yeh C-Y 2006 Synthesis, structure, and optical and electrochemical properties of star-shaped porphyrin–triarylamine conjugates *Org. Lett.* **8** 4239
62. D'Souza F, Gadde S, Islam D-M S, Wijesinghe C A, Schumacher A L, Zandler M E, et al. 2007 Multi-triphenylamine-substituted porphyrin-fullerene conjugates as charge stabilizing "antenna-reaction center" mimics *J. Phys. Chem. A* **111** 8552
63. Jain K, Duvva N, Badgurjar D, Giribabu L and Chitta R 2016 Synthesis and spectroscopic studies of axially bound tetra (phenothiazinyl)/tetra (bis (4′-tert-butylbiphenyl-4-yl) aniline)-zinc (II) porphyrin-fullero [C60 & C70] pyrrolidine donor–acceptor triads *Inorg. Chem. Commun.* **66** 5
64. Gangada S, Chakali M, Mandal H, Duvva N, Chitta R, Lingamallu G and Bangal P R 2018 Excitation-dependent electron exchange energy and electron transfer dynamics in a series of covalently tethered N, N-bis (4′-tert-butylbiphenyl-4-yl) aniline–[C60] fullerene dyads via varying π-conjugated spacers *Phys. Chem. Chem. Phys.* **20** 21352
65. Wienk M M and Janssen R A 1996 Stable triplet-state di (cation radical) s of a N-phenylaniline oligomer *Chem. Commun.* **2** 267
66. Stickley K R, Selby T D and Blackstock S C 1997 Isolable polyradical cations of polyphenylenediamines with populated high-spin states *J. Org. Chem.* **62** 448
67. Ishikawa M, Kawai M and Ohsawa Y 1991 Synthesis and properties of electrically conducting polytriphenylamines *Synth. Met.* **40** 231
68. Chang A Y, Chen Y-H, Lin H-W, Lin L-Y, Wong K-T and Schaller R D 2013 Charge carrier dynamics of vapor-deposited small-molecule/fullerene organic solar cells *J. Am. Chem. Soc.* **135** 8790
69. Komamine S, Fujitsuka M, Ito O, Moriwaki K, Miyata T and Ohno T 2000 Photoinduced charge separation and recombination in a novel methanofullerene–triarylamine dyad molecule *J. Phys. Chem. A* **104** 11497
70. Rajkumar G A, Sandanayaka A S, Ikeshita K-i, Itou M, Araki Y, Furusho Y, et al. 2005 Photoinduced intramolecular electron-transfer processes in [60] fullerene-(spacer)-N, N-bis (biphenylyl) aniline dyad in solutions *J. Phys. Chem. A* **109** 2428
71. Bang J H and Kamat P V 2011 CdSe quantum dot–fullerene hybrid nanocomposite for solar energy conversion: electron transfer and photoelectrochemistry *ACS Nano* **5** 9421
72. Suneel G, Ramya A R, Akanksha A S, Ravinder P, Jagadeesh B N, Parth R, et al. 2020 Excitation-wavelength-dependent light-induced electron transfer and twisted intramolecular charge transfer in *N,* N-Bis(4'-*ter*t-butylbiphenyl-4-yl)aniline functionalized borondipyrromethenes *J. Phys. Chem. A* **124** 9738
73. Duvva N, Gangada S, Chitta R and Giribabu L 2020 Bis(4′-tert-butylbiphenyl-4-yl)aniline (BBA)-substituted A_3B zinc porphyrin as light harvesting material for conversion of light energy to electricity *J. Porphyr. Phthalocyan.* **24** 1189
74. Grimme S, Bannwarth C and Shushkov P 2017 A robust and accurate tight-binding quantum chemical method for structures, vibrational frequencies, and noncovalent interactions of large molecular systems parametrized for all spd-block elements (Z = 1–86) *J. Chem. Theor. Comput.* **13** 1989
75. AMS DFTB 2020 *SCM, Theoretical Chemistry* (Vrije Universiteit: Amsterdam)
76. Gaussian 16, Revision C.01, Frisch M J, Trucks G W, Schlegel H B, Scuseria G E, Robb M A, Cheeseman J R, et al. 2016 Gaussian, Inc., Wallingford CT
77. Kanika J, Naresh D, Deepak B, Lingamallu G and Raghu C 2016 Synthesis and spectroscopic studies of axially bound tertra(phenothiazinyl)/tetra(bis(4'-tert-butylbiphenyl-4-yl)aniline)-zinc(II)porphyrin-fullero[C_{60} & C_{70}]pyrrolidine donor-acceptor triads *Inorg. Chem. Commun.* **66** 5
78. Raghu C, Deepak B, Govind R, Kanika J, Vijendar R K, Anjaiah B and Lingamallu G 2021 Light-induced energy transfer followed by electron transfer in axially co-ordinated benzothaizole tethered zinc porphyrin-fullero[C_{60}/C_{70}]pyrrolidine triads *J. Porphyr. Phthalocyan.* **25** 469